Supplementary Figures

Molecular and petrographical evidence for lacustrine environmental and biotic change in the palaeo-Sichuan mega-lake (China) during the Toarcian Oceanic Anoxic Event

Weimu Xu [a,b,*], Johan W.H. Weijers [c], Micha Ruhl [a,d], Erdem F. Idiz [a], Hugh C. Jenkyns [a], James B. Riding [e], Olga Gorbanenko [a], Stephen P. Hesselbo [f]

[a] Department of Earth Sciences, University of Oxford, Oxford OX1 3AN, UK

[b] School of Earth Sciences, University College Dublin, Belfield, Dublin 4, Ireland

[c] Shell Global Solutions International B.V., Shell Technology Centre Amsterdam, Grasweg 31, 1031 HW, Amsterdam, The Netherlands

[d] Department of Geology, Trinity College Dublin, The University of Dublin, College Green, Dublin 2, Ireland

[e] British Geological Survey, Keyworth, Nottingham NG12 5GG, UK

[f] Camborne School of Mines and Environment and Sustainability Institute, University of Exeter, Penryn Campus, Penryn, Cornwall TR10 9FE, UK

[*] Corresponding author: weimu.xu1@ucd.ie

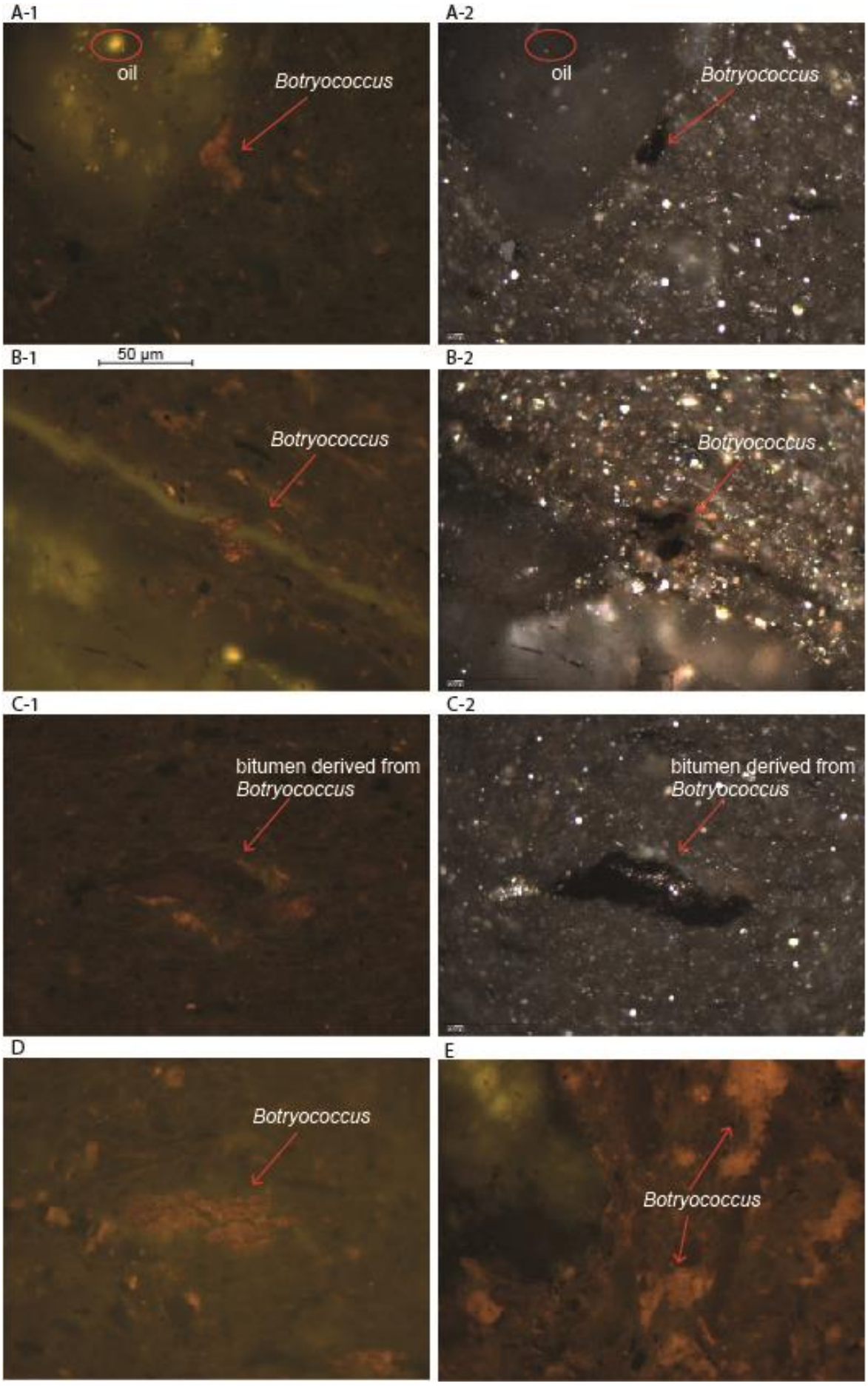
A-1
oil
Botryococcus
A-2
oil
Botryococcus
B-1
50 μm
Botryococcus
B-2
Botryococcus
C-1
bitumen derived from
Botryococcus
C-2
bitumen derived from
Botryococcus
D
Botryococcus
E
Botryococcus

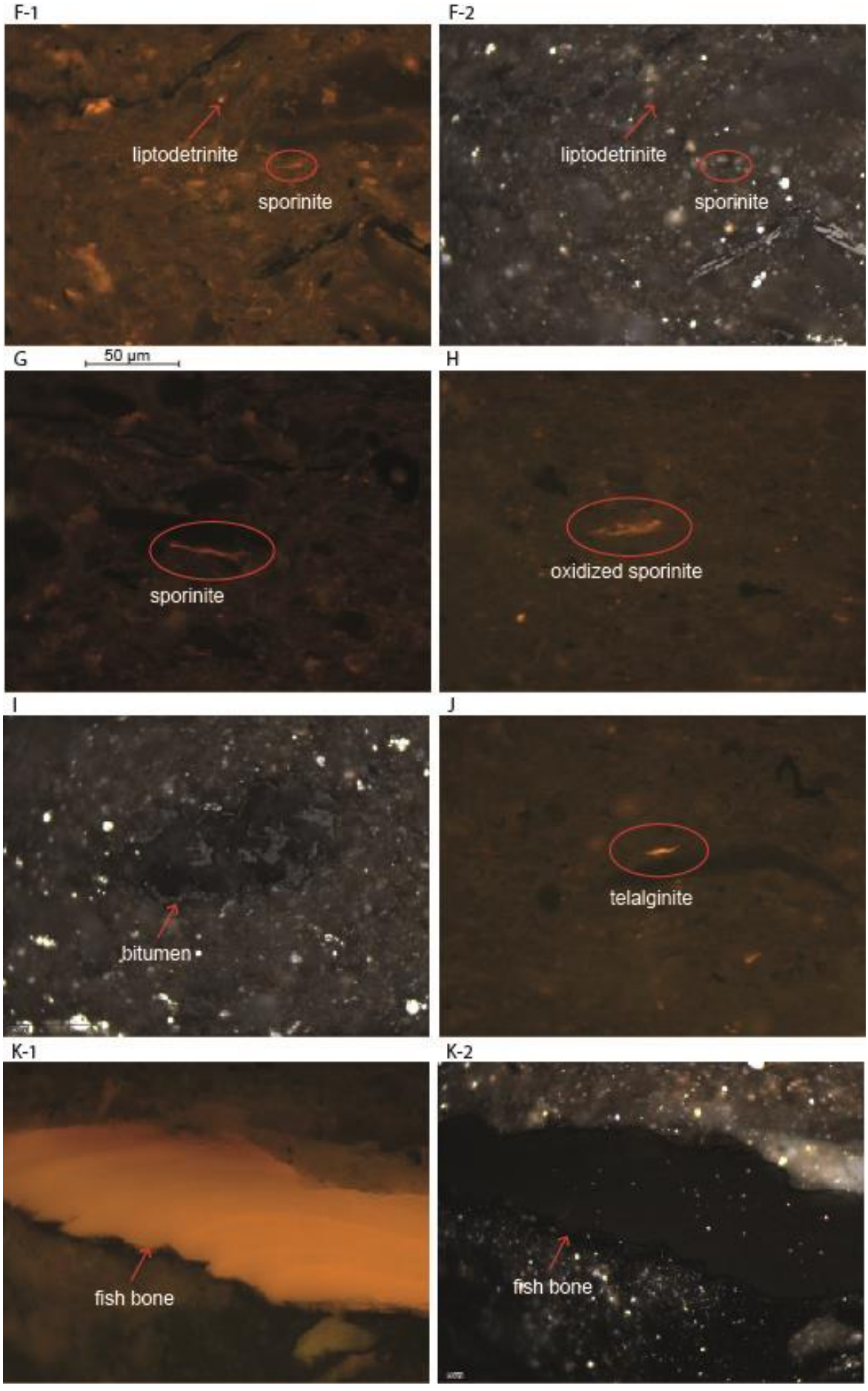
F-1
liptodetrinite
sporinite
F-2
liptodetrinite
sporinite
G
50 μm
sporinite
H
oxidized sporinite
I
bitumen
J
telalginite
K-1
fish bone
K-2
fish bone

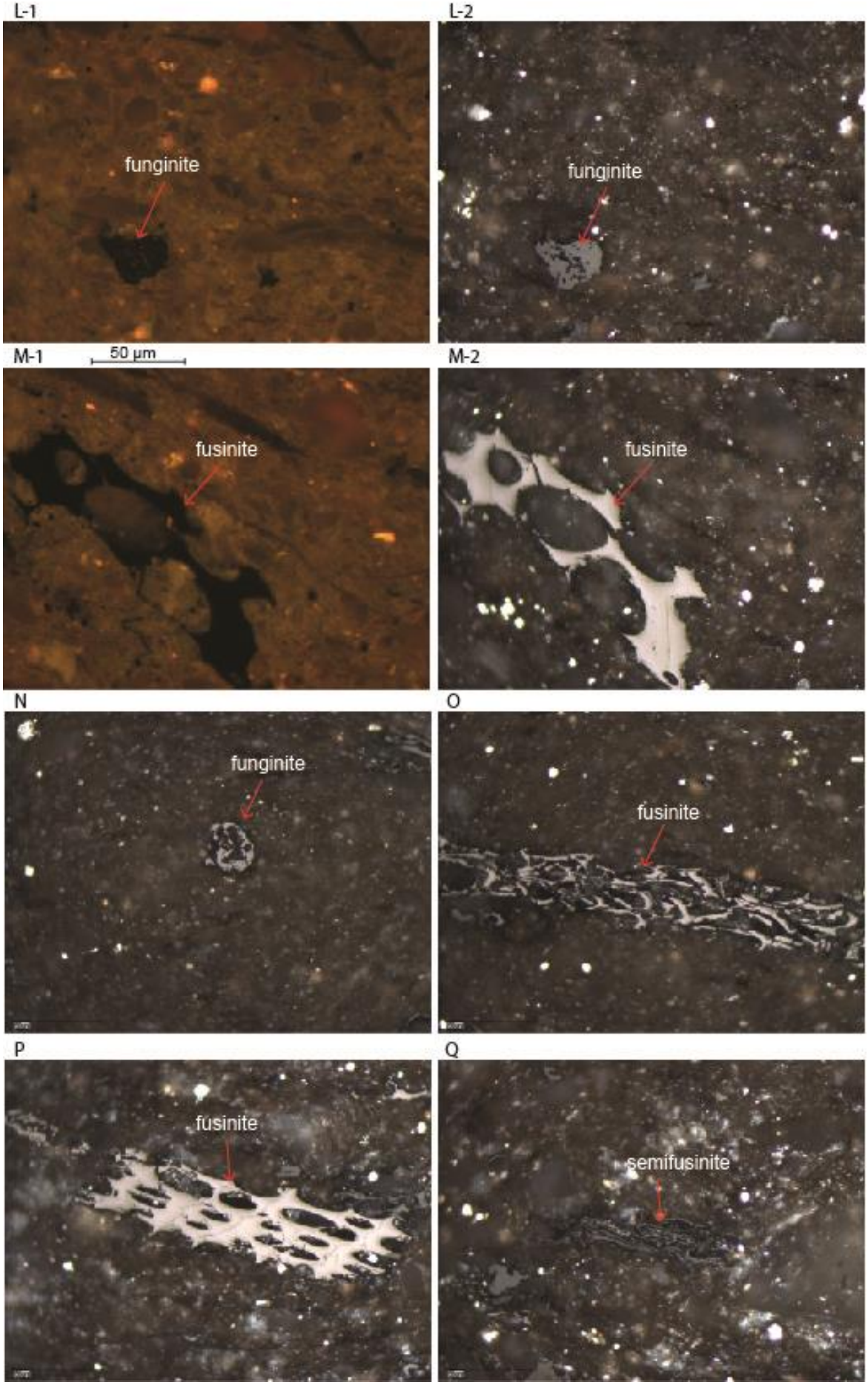
L-1
funginite
L-2
funginite
M-1
50 μm
fusinite
M-2
fusinite
N
funginite
O
fusinite
P
fusinite
Q
semifusinite

S_Fig. 1 Photos of different macerals from Core A (extended photos for Fig. 5 in the main text). Plate 1: Examples of telalginite (specifically *Botryococcus-derived*), showing an orange-yellow colour of moderate intensity in the UV light and dark grey-brownish colour in the reflected white light (in oil immersion). Photos A-1 and A-2: *Botryococcus*-derived telalginite close to oil droplets under UV and reflected white light (Core A: 2681.17 m); photos B-1 and B-2: *Botryococcus*-derived telalginite under UV and reflected white light (Core A: 2681.17 m); photos C-1 and C-2: bitumen originated from *Botryococcus* under UV and reflected white light (Core A: 2691.25 m); photo D: *Botryococcus*-derived telalginite under UV light (Core A: 2681.17 m); photo E: *Botryococcus*-derived telalginite close to oil droplets under UV light (Core A: 2702.13 m).

Plate 2: Examples of liptinite (sporinite, liptodetrinite, telalginite) and zooclast (fish bone) (oil immersion). Photos F-1 and F-2: sporinite and liptodetrinite in orange colour under UV light and dark grey under reflected white light (Core A: 2702.13 m); photo G: sporinite showing an orange colour under UV light (Core A: 2710.73 m); photo H: oxidized sporinite that is poorly preserved in orange-yellow colour under the UV light (Core A: 2691.25 m); photo I: bitumen showing a dark grey colour and low reflectance in reflected white light (Core A: 2702.13 m); photo J: telalginite in bright orange colour under UV light (Core A: 2691.25 m); photos K-1 and K-2: a relict of fish bone showing bright orange fluorescence under UV light and dark grey colour in reflected white light (Core A: 2681.17 m).

Plate 3: Examples of inertinite particles (fusinite, semifusinite and funginite) (under oil immersion). Photos L-1 and L-2: funginite particle showing a light grey colour under reflected white light and dark grey under UV light (Core A: 2710.73 m); photos M-1 and M-2: fusinite particle showing high-reflecting light grey colour under reflected white light and dark grey under UV light (Core A: 2710.73 m); photo N: funginite particle showing a light grey colour under reflected white light (Core A: 2691.25 m); photo O: fusinite particle

exhibiting a high-reflecting light grey colour under reflected white light (Core A: 2691.25 m); photo P: fusinite particle showing high-reflecting light grey colour under reflected white light (Core A: 2710.73 m); photo Q: semifusinite particle showing grey colour under reflected white light (Core A: 2710.73 m).

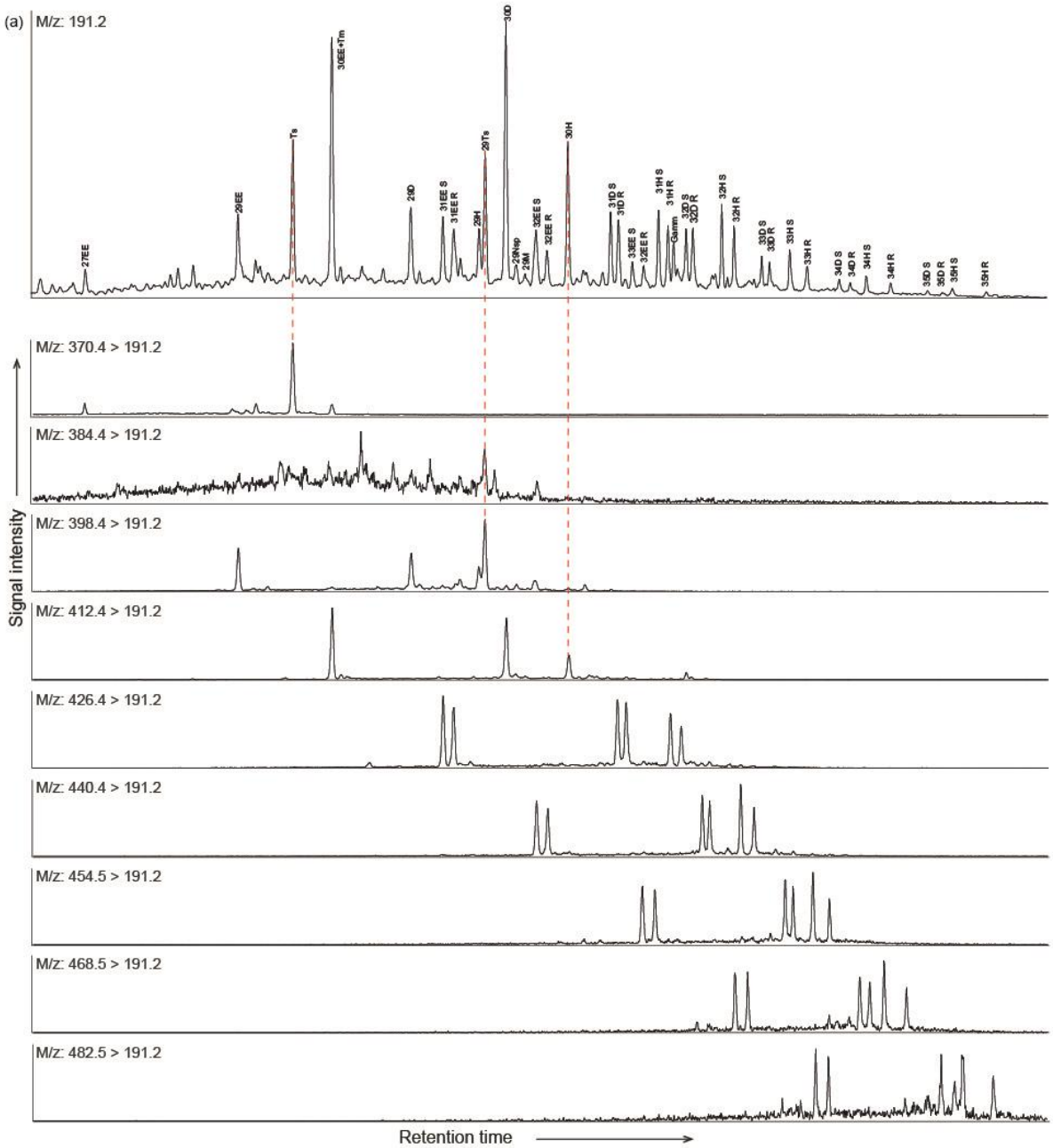

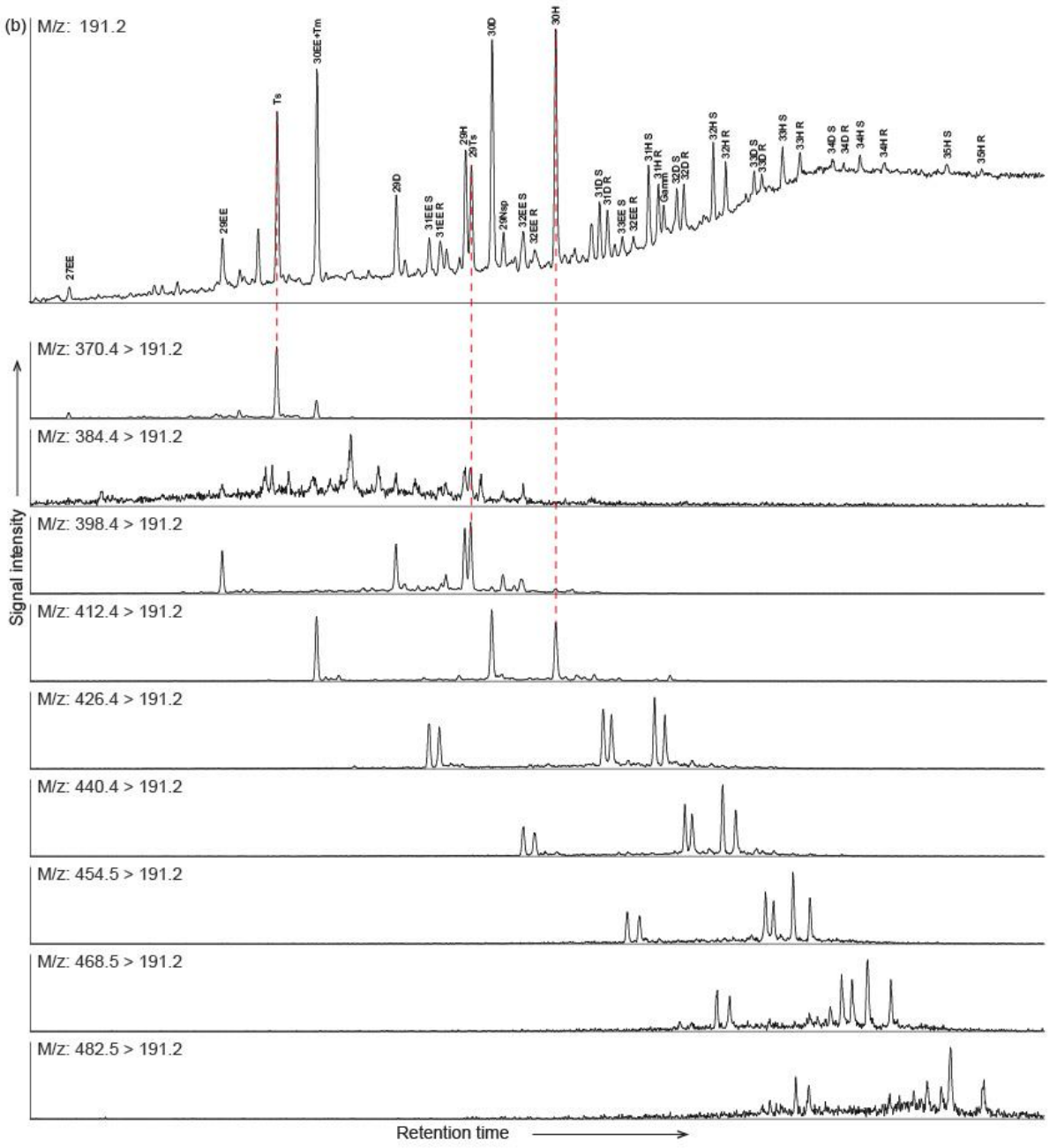
(b)
M/z: 191.2
27EE
29EE
Ts
30EE+Tm
29D
31EE S
31EE R
29H
29Ts
30D
29Nsp
32EE S
32EE R
30H
31D S
31D R
33EE S
32EE R
31H S
31H R
Gamm
32D S
32D R
32H S
32H R
33D S
33D R
33H S
33H R
34D S
34D R
34H S
34H R
35H S
35H R
M/z: 370.4 > 191.2
M/z: 384.4 > 191.2
M/z: 398.4 > 191.2
M/z: 412.4 > 191.2
M/z: 426.4 > 191.2
M/z: 440.4 > 191.2
M/z: 454.5 > 191.2
M/z: 468.5 > 191.2
M/z: 482.5 > 191.2
Signal intensity
Retention time

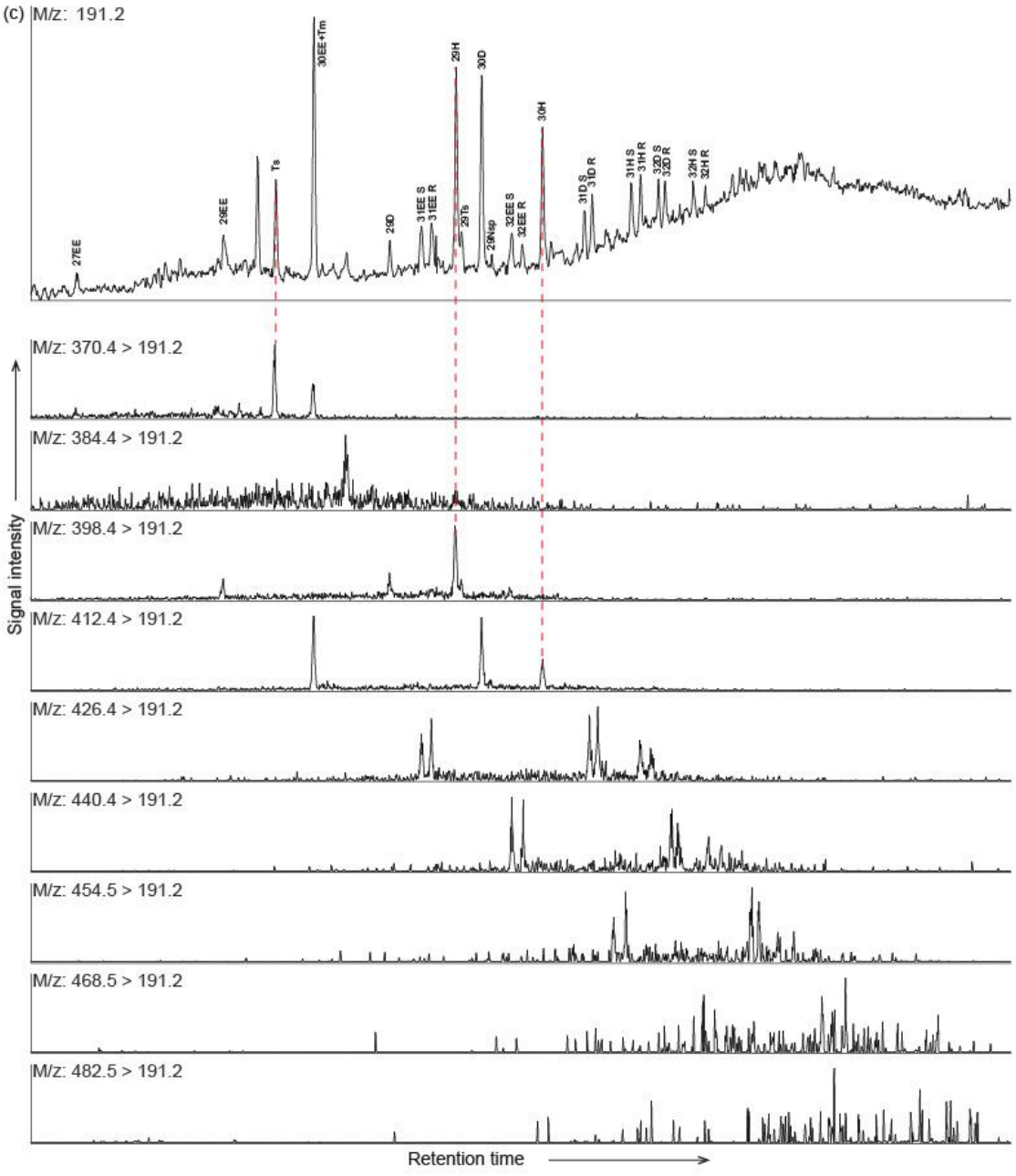

S_Fig. 2 Chromatogram of *m/z* 191 from GC/MS aligned with panels of mass chromatograms of C_{27}–C_{35} hopanes from GC/MSxMS data (extended chromatograms for Fig. 7 in the main text). (a) depth 2681.17 m (Core A); (b) depth 2702.13 m (Core A); (c) depth 3120.5 m (Core B). In the GC/MSxMS panels, the different transitions all have the same range for the *x*-axis and are all auto-scaled for the y-axis. Abbreviations: EE: early eluting hopane, D: diahopane, H: hopane, Gamm: Gammacerane.

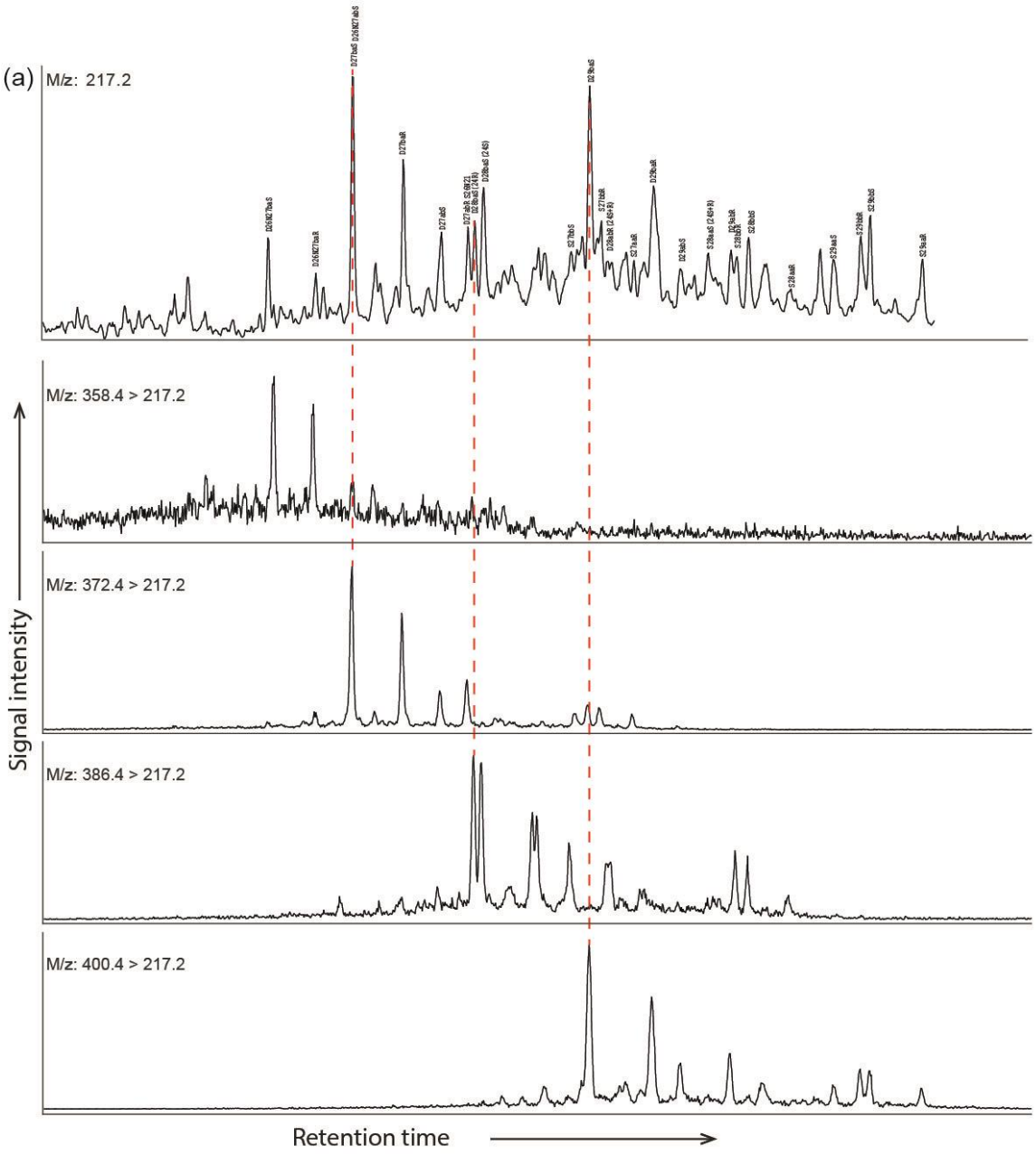
(a)
M/z: 217.2
M/z: 358.4 > 217.2
M/z: 372.4 > 217.2
M/z: 386.4 > 217.2
M/z: 400.4 > 217.2
Signal intensity
Retention time

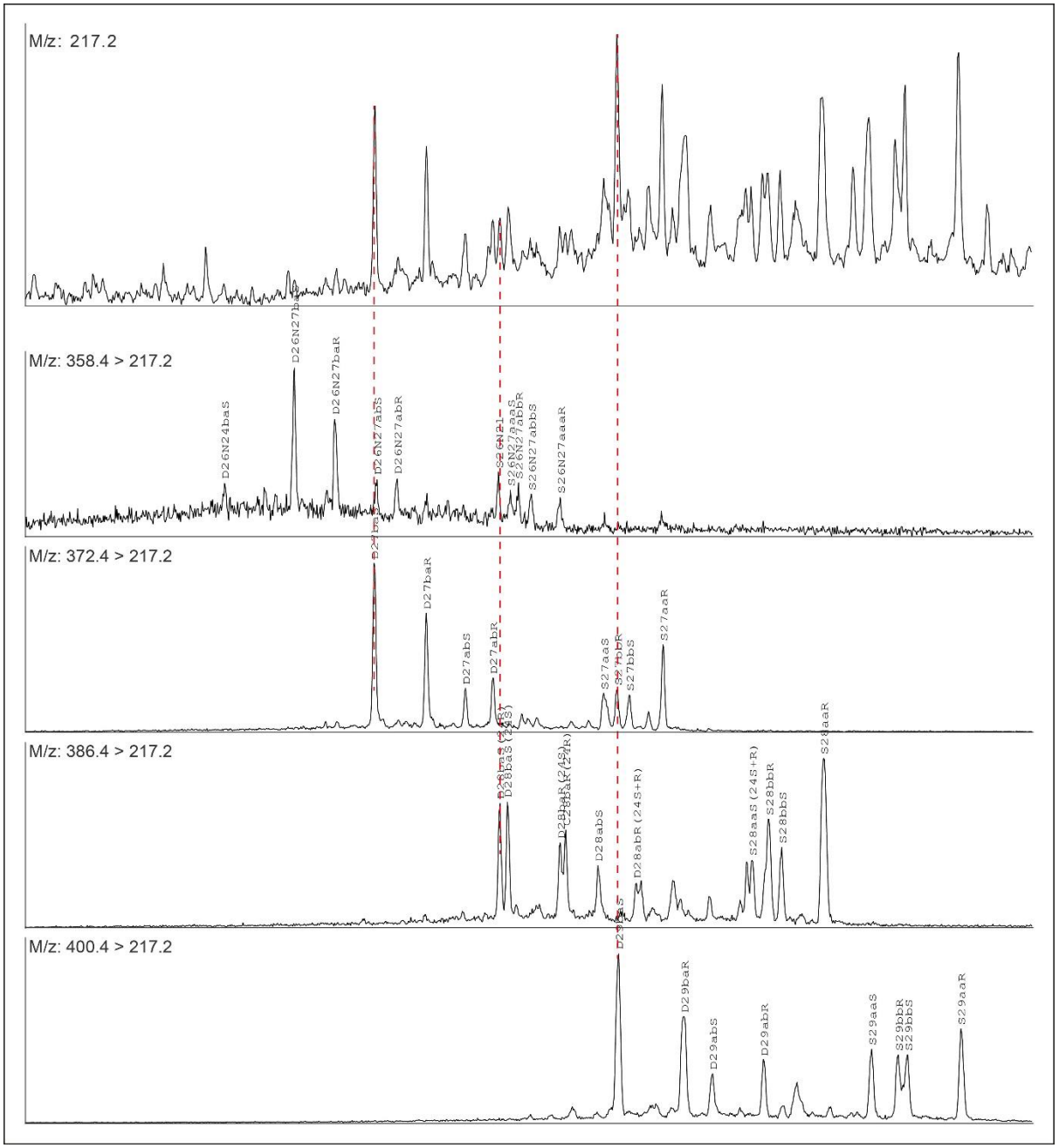
M/z: 217.2
M/z: 358.4 > 217.2
D26N24baS
D26N27baR
D26N27abS
D26N27abR
S26N21
S26N27aaS
S26N27abR
S26N27abbS
S26N27aaaR
M/z: 372.4 > 217.2
D27baR
D27abS
D27abR
S27aaS
S27abR
S27bbS
S27aaR
S28aaR
M/z: 386.4 > 217.2
D28baS (24S)
D28baR (24R)
D28abS
D28abR (24S+R)
S28aaS (24S+R)
S28bbR
S28bbS
M/z: 400.4 > 217.2
D29baR
D29abS
D29abR
S29aaS
S29bbR
S29bbS
S29aaR

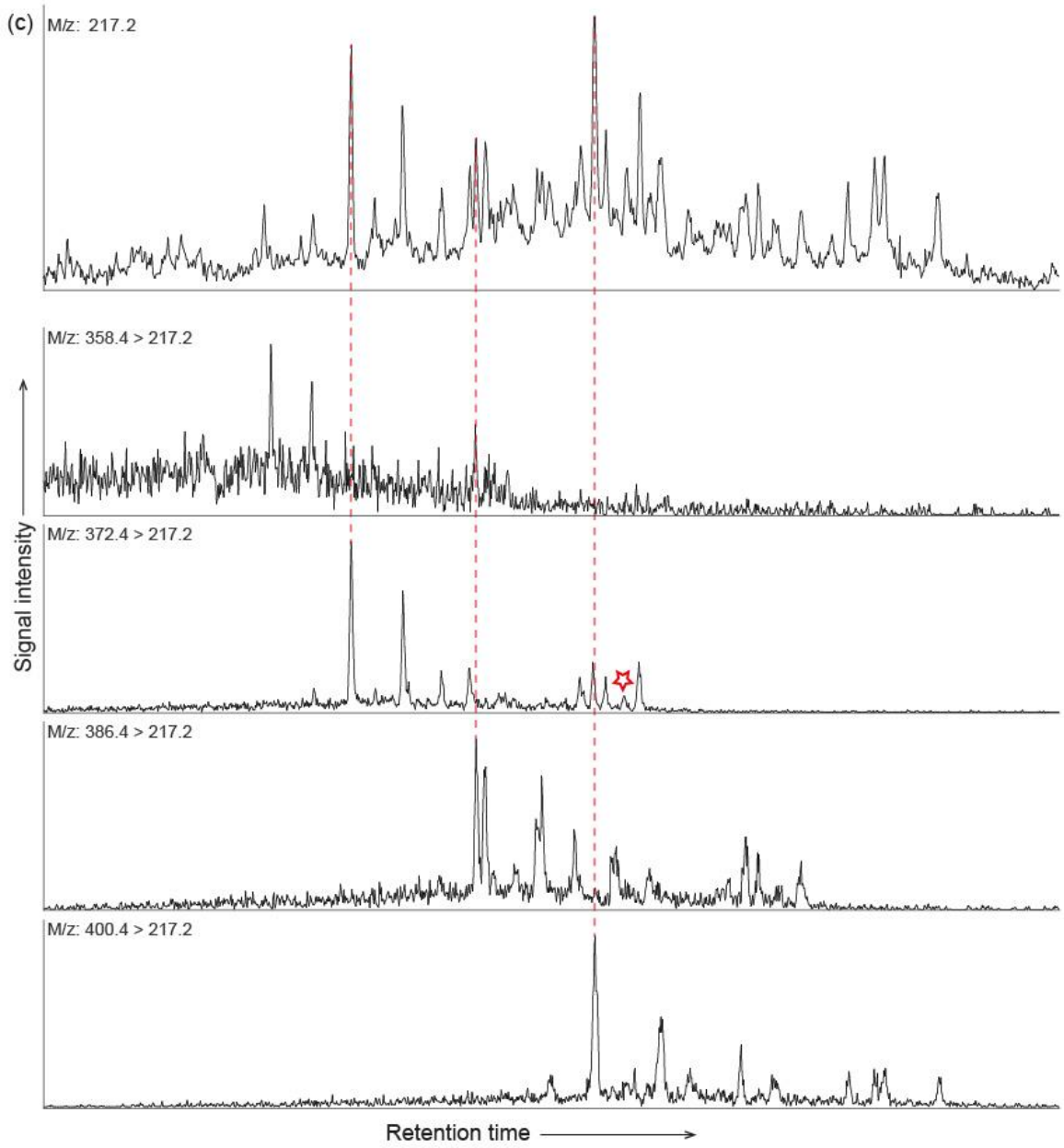

S_Fig. 3 Mass chromatogram of *m/z* 217 from GC/MS aligned with panels of chromatograms of C_{26}–C_{29} steranes from GC/MSxMS data (extended chromatograms for Fig. 8 in the main text). (a) depth 2681.17 m (Core A); (b) depth 2702.13 m (Core A); (c) depth 3120.5 m (Core B). In the GC/MSxMS panels, the different transitions all have the same range for the *x*-axis and are all auto-scaled for the y-axis. The red stars marked in the mass transition *m/z* 372→217 in (b) and (c) indicate the unknown peak.

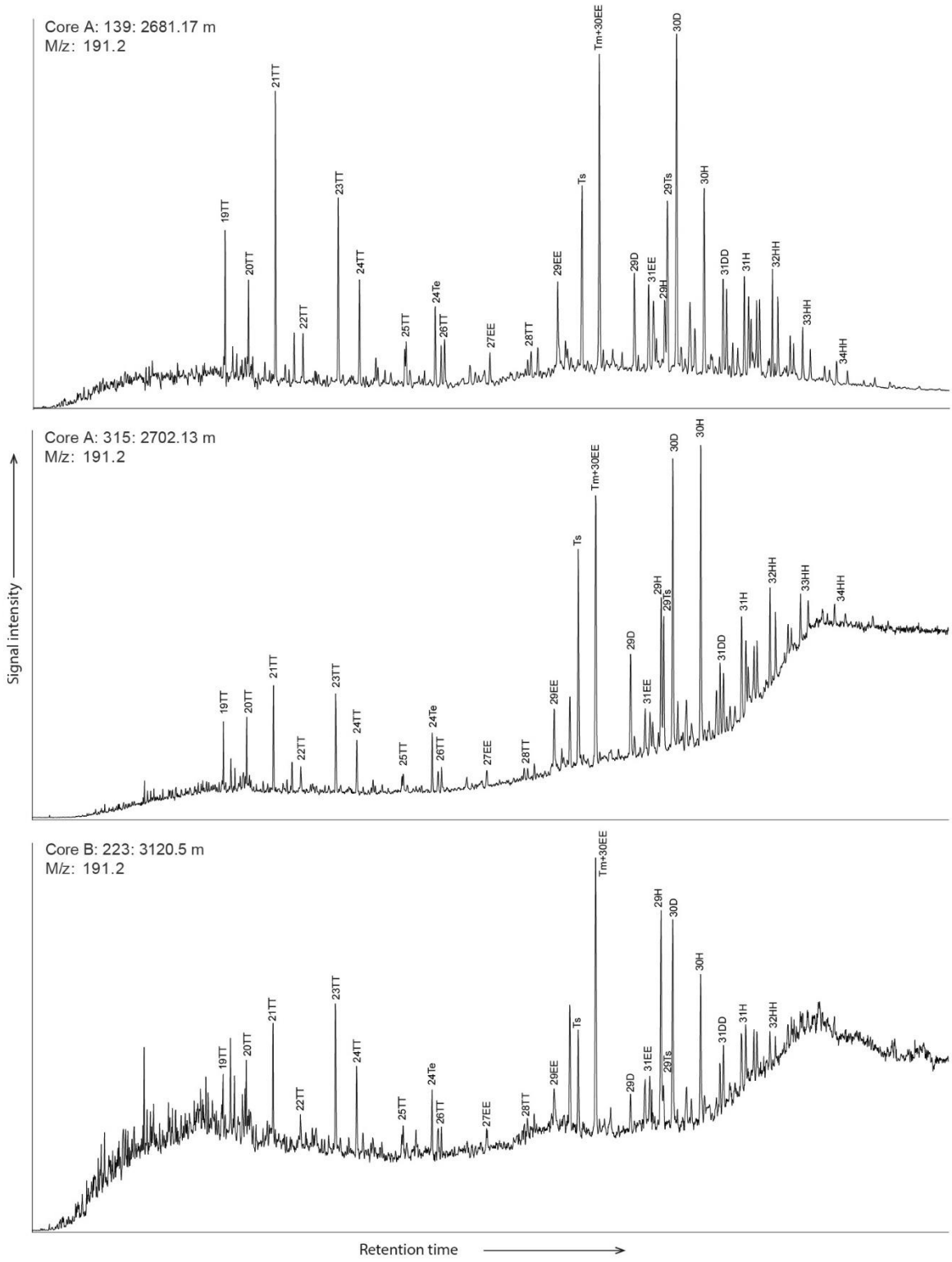

S_Fig. 4 GC/MS mass chromatogram of *m/z* 191 illustrating the tricyclic and pentacyclic terpanes. 19TT to 26TT represent tricyclic terpanes of C_{19}–C_{26}; 24Te represents C_{24} tetracyclic terpane. Abbreviations are as in supplementary Fig. 2

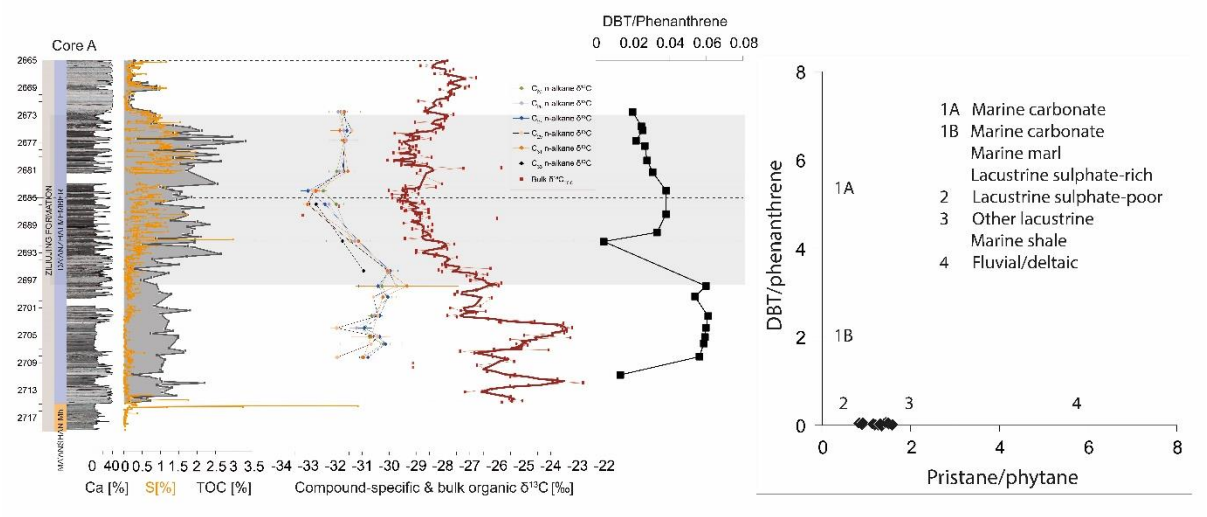

S_Fig. 5 DBT/Phenanthrene ratios over the studied interval, plotted against TOC, S content, $\delta^{13}C_{TOC}$ and $\delta^{13}C_{n\text{-alkanes}}$ from Xu et al. (2017), for the Da'anzhai Member of Core A on the left; DBT/Phenanthrene ratios *vs* Pristane/phytane ratios on the right (following Hughes et al., 1995).